JOURNAL OF SOLID STATE CHEMISTRY 108, 51–58 (1994)

Synthesis, Structures, and Characterization of MMnZrF$_7$ (M = Tl, Rb, NH$_4$, K) Fluorides: An Example of 7-Coordination of Divalent Manganese

Malika El-Ghozzi,* Daniel Avignant,*,[1] and Maurice Guillot†

*Laboratoire de Chimie des Solides, URA 444 du CNRS, Université Blaise Pascal, 63177 Aubière Cedex, France; and †Service National des Champs Intenses, CNRS, BP 166X, 38042 Grenoble Cedex, France

Received August 24, 1992; in revised form April 20, 1993; accepted April 22, 1993

A series of phases with formula M^1MnZrF$_7$ (M^1 = Tl, Rb, NH$_4$, K) was synthesized and their crystal chemical characteristics were determined from X-ray powder diffraction data. The structures of both Tl and Rb representatives were refined from single crystal X-ray diffraction data. Both Tl and Rb fluorides are isostructural and crystallize in the monoclinic system with unit cell dimensions a = 6.450(1) Å, b = 8.250(1) Å, c = 6.459(2) Å, β = 118.0(2)° and a = 6.439(3) Å, b = 8.218(2) Å, c = 6.443(1) Å, β = 117.9(2)° respectively, $P2_1/m$ (No. 11) space group, Z = 2. This structural type is built of chains of edge-shared alternated pentagonal bipyramids of Mn^{2+} and Zr^{4+} extending along the [1 0 1] direction, chains that are linked together by sharing corners to form $(MnZrF_7)_n^{n-}$ layers perpendicularly to the b axis. Layers are connected through apical fluorine atoms of the pentagonal bipyramidal groups, into a three-dimensional network delimiting pseudohexagonal tunnels parallel to the [0 1 0] direction, within which the M^1 monovalent cations are located. Structural relationships with KIn$_2$F$_7$, β-KYb$_2$F$_7$ and β-U$_3$O$_8$ structures are discussed.

INTRODUCTION

Within the general framework of the research dealing with the crystal chemistry of tetravalent zirconium in fluorinated or oxyfluorinated medium (1–6), we have carried out a study of the TlF–MnF$_2$–ZrF$_4$ ternary system using X-ray diffraction and DTA experiments. This work allowed us to characterize a new compound corresponding to an equimolar mixture of the TlF, MnF$_2$, and ZrF$_4$ starting materials leading to the TlMnZrF$_7$ formula. As Babel and co-workers (7) emphasized some time ago, an interesting feature concerning the diversity of polyhedral networks encountered in the crystal chemistry of heptafluorodimetallates, we have undertaken the crystal structure determination of both Tl and Rb representatives of MMnZrF$_7$ (M = Tl, Rb, NH$_4$, K) fluorides. In this paper we report their crystal structures determinated from single crystal X-ray diffraction data and the crystal chemical characterization of NH$_4$MnZrF$_7$ and KMnZrF$_7$ as well as results of a magnetic study of TlMnZrF$_7$.

[1] To whom correspondence should be addressed.

EXPERIMENTAL

Polycrystalline samples of MMnZrF$_7$ (M = Tl, Rb, NH$_4$, K) compounds were prepared by reacting stoichiometric quantities of the starting materials in platinum tubes sealed under dry argon gas. Two heating treatments of 12 hr with intermittent grinding were necessary to obtain pure samples. The ammonium ones were heated at 400°C whereas the others were prepared at 450°C. All samples were cooled down to room temperature slowly at the end of each heating treatment. Some of the starting materials were prepared in the laboratory. The thallous fluoride was obtained by incomplete neutralization of a 40% aqueous HF boiling solution by thallous carbonate followed by an evaporation to dryness. The dry extract was ground and then heated for a few hours at 200°C under a dry argon flow in order to remove remaining traces of water and hydrofluoric acid. The zirconium tetrafluoride was prepared by direct fluorination of pure ZrO$_2$ (Merck reagent grade) by heating it twice in F$_2$ gas overnight at 500°C with intermittent grinding of the samples. The manganese difluoride was obtained very pure by thermal decomposition of the NH$_4$MnF$_3$ complex at 200°C under vacuum. NH$_4$MnF$_3$ itself was prepared as a white precipitate by slowly adding MnO oxide (reagent grade) to a 50% aqueous HCl hot solution and then NH$_4$F (reagent grade).

Prior to use, both KF and RbF (Merck, selectipur) were heated at 500°C under vacuum in order to remove traces of water.

Single crystals of these MMnZrF$_7$ (M = Tl, Rb, NH$_4$, K) phases suitable for X-ray structure determination were obtained by slowly evaporating to dryness a 40% aqueous

0022-4596/94 $6.00

HF solution to which polycrystalline samples synthesized in the solid state were added as this solution was brought to the boil. Small colorless plate-like crystals were extracted from the dry residue. They were identified as such by comparison between the X-ray powder diffraction patterns obtained from ground specimens and those from samples prepared in the solid state; the pattern of the archetype $TlMnZrF_7$ is given in Table 1.

DTA experiments were carried out using a Netzsch thermal analyzer equipped with a 1550°C DDK probe. All experiments were performed on polycrystalline samples previously annealed at adequate temperatures. Magnetic measurements were performed at the High Field Magnet Laboratory in Grenoble on polycrystalline samples according to the extraction method and using a device described elsewhere (8).

TABLE 1
X-Ray Powder Pattern of $TlMnZrF_7$

d_{obs} (Å)	d_{calc} (Å)	h	k	l	I/I_0
5.69	5.69	1	0	0	32
		0	0	1	
5.52	5.52	$\bar{1}$	0	1	5
4.689	4.686	1	1	0	8
	4.685	0	1	1	
4.586	4.586	$\bar{1}$	1	1	4
4.126	4.124	0	2	0	3
3.336	3.340	1	2	0	100
		0	2	1	
3.308	3.303	$\bar{1}$	2	1	62
3.220	3.219	$\bar{2}$	0	1	66
	3.218	$\bar{1}$	0	2	
2.8463	2.8475	2	0	0	6
	2.8466	0	0	2	
2.7575	2.7587	$\bar{2}$	0	2	8
2.5887	2.5878	1	2	1	7
2.5371	2.5374	$\bar{2}$	2	1	15
	2.5369	$\bar{1}$	2	2	
2.4768	2.4758	1	3	0	3
	2.4756	0	3	1	
2.3429	2.3432	2	2	0	29
	2.3426	0	2	2	
2.2924	2.2929	$\bar{2}$	2	2	17
2.1216	2.1232	$\bar{3}$	0	1	16
	2.1224	$\bar{1}$	0	3	
2.0620	2.0619	0	4	0	20
1.9388	1.9387	1	4	0	7
	1.9386	0	4	1	
1.9216	1.9222	2	2	1	22
	1.9219	1	2	2	
1.8973	1.8984	3	0	0	21
	1.8977	0	0	3	
1.8664	1.8676	$\bar{3}$	2	2	26
	1.8673	$\bar{2}$	2	3	
1.8385	1.8391	$\bar{3}$	0	3	11
1.7523	1.7521	1	4	1	13
1.7362	1.7362	$\bar{2}$	4	1	20
	1.7360	$\bar{1}$	4	2	
1.6624	1.6619	2	0	2	8
1.6516	1.6515	$\bar{2}$	4	2	4
1.6084	1.6095	$\bar{4}$	0	2	7
	1.6089	$\bar{2}$	0	4	
1.5338	1.5340	$\bar{4}$	0	3	6
	1.5337	$\bar{3}$	0	4	
1.4986	1.4993	$\bar{4}$	2	2	4
	1.4989	$\bar{2}$	2	4	
1.4844	1.4847	3	2	1	8
	1.4844	1	2	3	
1.4803	1.4792	$\bar{3}$	4	1	9
	1.4789	$\bar{1}$	4	3	
1.4625	1.4623	$\bar{4}$	2	1	10
	1.4618	$\bar{1}$	2	4	
1.4375	1.4377	$\bar{4}$	2	3	4
	1.4375	$\bar{3}$	2	4	
1.4239	1.4238	4	0	0	4
	1.4233	0	0	4	
1.3968	1.3966	3	4	0	12
	1.3963	0	4	3	
1.3729	1.3725	$\bar{3}$	4	3	6
1.3457	1.3458	4	2	0	4
	1.3454	0	2	4	
1.3349	1.3338	$\bar{1}$	6	1	6
1.3082	1.3081	$\bar{4}$	2	4	4
1.2946	1.2939	2	4	2	5
1.2848	1.2847	$\bar{5}$	0	2	3
	1.2843	$\bar{2}$	0	5	
1.2690	1.2694	$\bar{5}$	1	2	6
	1.2690	$\bar{2}$	1	5	
	1.2687	$\bar{4}$	4	2	
	1.2684	$\bar{2}$	4	4	

RESULTS

Basic characterization:

The X-ray powder pattern of the archetype $TlMnZrF_7$ is given in Table 1. Wherease Tl, Rb, and NH_4 compounds patterns could have been indexed on the basis of a monoclinic cell determined from a single crystal (see next section), the K compound pattern has been indexed by isotypy with the KIn_2F_7 fluoride (9). The lattice parameters of these compounds are given in Table 2. Figure 1 displays the variation of the volume of the formula unit versus the cube of the ionic radius of the M^I monovalent element in the M^IMnZrF_7 series. From this plot based on lattice

TABLE 2
Lattice Parameters of M^IMnZrF_7 Phases

	Space group	a (Å)	b (Å)	c (Å)	β (°)	Z
$TlMnZrF_7$	$P2_1/m$	6.443(3)	8.247(2)	6.441(3)	117.9(1)	2
$RbMnZrF_7$	$P2_1/m$	6.416(2)	8.248(2)	6.418(1)	117.7(1)	2
NH_4MnZrF_7	$P2_1/m$	6.420(2)	8.219(3)	6.415(4)	117.7(1)	2
$KMnZrF_7$	$P2_1/m$	10.755(1)	8.153(2)	6.629(2)	90.4(1)	4

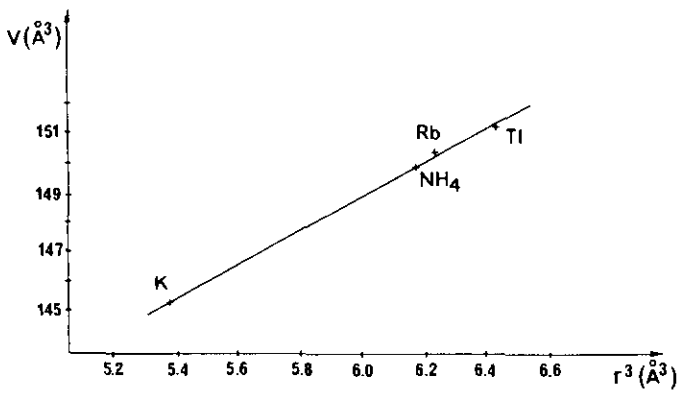

FIG. 1. Variation of the formula unit volume versus the cube of the ionic radius of M^I monovalent element in M^IMnZrF$_7$ fluorides series.

parameters given in Table 2, it should be pointed out that in spite of the difference in unit cell between K and the other monovalent ions of larger size, this variation is straightforward. It may thus be concluded that both variants related to this structural type have quite similar compactnesses.

STRUCTURE DETERMINATION AND REFINEMENT

TlMnZrF$_7$

A small colorless crystal with a rectangular platelet-like shape was mounted on a pyrex rod using epoxy paste. Unit cell dimensions were determined accurately using a four-circle Nonius CAD4 diffractometer by centering on 25 reflections with $20° \leq 2\theta \leq 60°$ and least squares refinement of the measured setting angles.

At the end of the data collection the conditions of which are given in Table 3, Lorentz and polarization corrections were applied, followed by an empirical absorption correction deduced from psi scan series on $\bar{1}$ 0 1, 0 2 0 and 1 4 1 reflections. The thallium atom location was deduced from the Patterson function and calculation of structure factors resulted in $R = 0.31$. Then a Fourier synthesis

TABLE 3
Crystallographic Data and Data Collection Parameters for TlMnZrF$_7$ and RbMnZrF$_7$

	I	II
Chemical formula	TlMnZrF$_7$	RbMnZrF$_7$
Symmetry	monoclinic	monoclinic
Space group	$P2_1/m$ (No. 11)	$P2_1/m$ (No. 11)
Unit cell parameters:		
a (Å)	6.450(1)	6.439(3)
b (Å)	8.250(1)	8.218(2)
c (Å)	6.459(2)	6.443(1)
β (°)	118.0(2)	117.9(2)
Z	2	2
ρ calc. (g/cm^3)	5.31	4.02
Crystal size (mm)	0.025 × 0.02 × 0.06	0.02 × 0.03 × 0.09
Radiation	Mo$K\alpha$ (λ = 0.71069 Å) graphite monochromated	Mo$K\alpha$ (λ = 0.71069 Å) graphite monochromated
μ (Mo$K\alpha$) (cm^{-1})	305.5	115.9
Transmission factors	0.68–0.99	0.78–0.99
Scan:		
mode	ω–2θ	ω–2θ
scan width	(0.80 + 0.35 tan θ)°	(0.80 + 0.35 tan θ)°
aperture	(2.70 + 0.40 tan θ) mm	(2.70 + 0.40 tan θ) mm
Range measured	$1 \leq \theta \leq 40$	$1 \leq \theta \leq 40$
	$-11 \leq h \leq 11$	$-11 \leq h \leq 11$
	$0 \leq k \leq 14$	$0 \leq k \leq 14$
	$0 \leq l \leq 11$	$0 \leq l \leq 11$
Period of intensity control	3600 sec, σ = 0.02	3600 sec, σ = 0.02
Number of measured reflections	100 reflections, σ = 0.10	100 reflections, σ = 0.10
Number of weak reflections	1963	1955
Number of observed reflections with $I > 3\sigma(I)$	1082	1173
	562	403
Number of variables	45	33
Weighting scheme	$\omega_i = 1/(\sigma^2(F) + 0.011096F^2)$	$\omega_i = 1/(\sigma^5(F) + 0.010404F^2)$
Function minimized	$R\omega = [\Sigma\omega(\lvert F_o\rvert - \lvert F_c\rvert)^2/\Sigma\omega(F_o)^2]^{1/2}$	
Secondary extinction parameter	3.33×10^{-8}	3.36×10^{-7}
Residuals	R = 0.038	R = 0.064
	R_w = 0.043	R_w = 0.074

TABLE 4
Atomic Coordinates and Thermal Parameters for $TlMnZrF_7$

Atoms	Wyckoff position	x	y	z	B_{iso} or B_{eq} (Å^2)
Tl	2c	0	0.5	0.5	2.18
Mn	2e	0.3157(7)	0.75	0.1878(6)	1.57
Zr	2e	0.3098(2)	0.25	0.1893(2)	0.32
F(1)	2e	0.5110(55)	0.25	0.0038(48)	2.84
F(2)	2e	0.3445(32)	0.25	0.5348(31)	3.16
F(3)	2e	0.3360(19)	0.75	0.5466(19)	0.94
F(4)	2e	0.0477(22)	0.25	0.8440(21)	1.17
F(5)	2e	0.0391(31)	0.75	0.8349(26)	3.06
F(6)	4f	0.3052(13)	0.0013(23)	0.1995(13)	2.20

Anisotropic thermal parameters (Å^2 × 10^4)[a]

	β_{11}	β_{22}	β_{33}	β_{12}	β_{13}	β_{23}
Tl	239	59	214	−34	33	−28
Mn	154	39	58	0	−84	0
Zr	14	11	32	0	41	0
F(1)	76	235	56	0	4	0
F(5)	188	220	59	0	4	0

[a] Aniosotropic temperature factors are of the form: $\exp[-2\pi^2(h^2U_{11}a^{*2} + \ldots + 2hkU_{12}a^*b^* + \ldots)]$.

enabled both zirconium and manganese atoms to be located. Two subsequent cycles of refinement of the cationic position led to a R value of 0.157. With these data a difference Fourier synthesis revealed the position of the six independent fluorine atoms. Subsequent full matrix least squares refinements and use of isotropic thermal parameters gave $R = 0.061$. The scattering factors for Tl^+, Zr^{4+}, Mn^{2+}, and F^- ions were taken from the International Tables for X-ray Crystallography (10), as were the anomalous dispersion terms for Tl and Zr for the Mo$K\alpha$ radiation. Final refinement including anisotropic thermal parameters for cations and for both F(1) and F(5) converged to $R = 0.038$ and $R_w = 0.043$ for 45 variables and 562 reflections. Final positional and thermal parameters are listed in Table 4.

$RbMnZrF_7$

A small colorless single crystal with a platelet-like habit was used for this study. As previously, the unit cell dimensions were determined by least squares refinement of the measured setting angles of 25 reflections with $20° \leq 2\theta \leq 60°$. This preliminary study showed that $RbMnZrF_7$ unit cell is quite similar to that of $TlMnZrF_7$.

Intensity measurements were recorded for the asymmetric unit corresponding to the $-11 \leq h \leq 11$, $0 < k \leq 14$, and $0 \leq l \leq 11$ range, with conditions mentioned in Table 3. Data were corrected for Lorentz and polarization effects and an empirical absorption correction deduced from four series of psi scan on 1 0 1, $\bar{1}$ 4 2, 0 4 0 and 0 4 3 reflections was applied to all intensities.

The structure of $RbMnZrF_7$ was solved, assuming that both Rb and Tl might be similar starting with the positional parameters determined for $TlMnZrF_7$. A few cycles of least squares refinements including anisotropic thermal parameters for the rubidium converged to $R = 0.064$ and $R_w = 0.074$ for 33 variables and 403 reflections. The largest peak in the final difference electron density map corresponds to 4.07 e/Å^3.

Final positional and thermal parameters are given in Table 5. All computer programs used for data collection, reduction, and refinement were from the CAD4 SDP package (11).

DESCRIPTION OF THE STRUCTURE AND DISCUSSION

In this structural type, both Zr^{4+} and Mn^{2+} ions are surrounded by seven F^- forming relatively regular pentagonal bipyramids as shown by selected bond distances and angles listed in Tables 6a and 6b. Within the zirconium coordination polyhedra, the Zr–F distances spread over the 2.05–2.18 and 2.03–2.15 Å ranges with mean values of 2.11 and 2.09 Å for the Tl and Rb compounds, respectively. These values are in good agreement with the sum of the ionoic radii of Shannon and Prewitt (12), namely 2.11 Å. Let us point out that in the β-$BaZr_2F_{10}$ fluoride (13), where a 7-coordinated Zr^{4+} ion is also pentagonal bipyramidal, a mean Zr–F distance of 2.05 Å has been found while the Zr–F distances spread over the 1.93–2.17 Å range. Let us also remember that in the $Rb_5Zr_4F_{21}$ compound (14) where a 7-coordination of the Zr^{4+} ion was

TABLE 5
Atomic Coordinates and Thermal Parameters for $RbMnZrF_7$

Atoms	Wyckoff position	x	y	z	B_{iso} or B_{eq} (Å^2)
Rb	2c	0	0.5	0.5	2.61
Mn	2e	0.3187(9)	0.75	0.1801(9)	1.63
Zr	2e	0.3085(4)	0.25	0.1921(4)	0.15
F(1)	2e	0.4801(69)	0.25	0.0167(74)	2.34
F(2)	2e	0.3507(33)	0.25	0.5366(32)	1.68
F(3)	2e	0.3301(31)	0.75	0.5418(31)	1.56
F(4)	2e	0.0492(30)	0.25	0.8425(30)	1.30
F(5)	2e	0.0302(33)	0.75	0.8377(34)	1.86
F(6)	4f	0.2981(18)	0.0028(34)	0.2004(17)	1.72

Anisotropic thermal parameters (Å^2 × 10^4)[a] for Rb

	β_{11}	β_{22}	β_{33}	β_{12}	β_{13}	β_{23}
Rb	243	68	257	−14	305	39

[a] Aniosotropic temperature factors are of the form: $\exp[-2\pi^2(h^2U_{11}a^{*2} + \ldots + 2hkU_{12}a^*b^* + \ldots)]$.

TABLE 6a
Selected Interatomic Distances (Å) in TlMnZrF$_7$

Tl–F(3)	2.90(1)	×2	F(1)–F(5)	2.58(3)
Tl–F(5)	2.91(1)	×2	F(1)–F(3)	2.59(3)
Tl–F(4)	2.94(1)	×2	F(1)–F(4)	2.66(4)
Tl–F(2)	2.96(2)	×2	F(1)–F(2)	2.70(3)
Tl–F(6)	3.35(1)	×6	F(1)–F(6)	2.98(3)
			F(1)–F(6)	3.02(3)
Mn–F(1)	2.02(3)		F(2)–F(3)	2.35(3)
Mn–F(2)	2.18(2)		F(2)–F(5)	2.50(2)
Mn–F(6)	2.08(2)	×2	F(2)–F(6)	2.91(2)
Mn–F(5)	2.13(1)		F(2)–F(6)	2.95(2)
Mn–F(4)	2.24(2)		F(3)–F(4)	2.57(1)
Mn–F(3)	2.25(2)		F(3)–F(6)	2.95(2)
⟨Mn–F⟩ = 2.14			F(3)–F(6)	2.99(2)
Zr–F(6)	2.05(2)	×2	F(4)–F(6)	2.94(2)
Zr–F(4)	2.07(1)		F(4)–F(6)	2.99(2)
Zr–F(3)	2.11(1)		F(5)–F(6)	2.95(2)
Zr–F(1)	2.14(4)		F(5)–F(6)	3.00(2)
Zr–F(2)	2.14(2)			
Zr–F(5)	2.18(2)			
⟨Zr–F⟩ = 2.11				
F(1)^{ii}–Mn–F(3)^{i}	147.8(7)		F(4)^{ii}–Mn–F(2)^{ii}	135.1(8)
F(1)^{ii}–Mn–F(4)^{ii}	142.7(7)		F(5)^{i}–Mn–F(2)^{ii}	159.(1)
F(3)^{i}–Mn–F(5)^{i}	135.4(7)		F(6)^{i}–Mn–F(6)^{iv}	173.2(5)
F(1)^{i}–Zr–F(5)^{ii}	146.8(7)		F(3)^{ii}–Zr–F(5)^{ii}	138.2(6)
F(1)^{i}–Zr–F(2)^{i}	142.3(8)		F(4)^{i}–Zr–F(2)^{i}	139.2(7)
F(3)^{ii}–Zr–F(4)^{i}	153.5(6)		F(6)^{i}–Zr–F(6)^{iv}	175.3(4)

Note. Symmetry codes: (i) (x, y, z), (ii) $(\bar{x}, \bar{y}, \bar{y})$, (iii) $(\bar{x}, \frac{1}{2} + y, \bar{z})$, and (iv) $(x, \frac{1}{2} - y, z)$.

TABLE 6b
Selected Interatomic Distances (Å) in RbMnZrF$_7$

Rb–F(3)	2.88(2)	×2	F(1)–F(4)	2.49(5)
Rb–F(4)	2.92(1)	×2	F(1)–F(2)	2.59(5)
Rb–F(5)	2.93(2)	×2	F(1)–F(3)	2.71(5)
Rb–F(2)	2.98(2)	×2	F(1)–F(5)	2.81(5)
Rb–F(6)	3.30(1)	×6	F(1)–F(6)	3.00(5)
			F(1)–F(6)	3.06(5)
Mn–F(1)	2.02(6)		F(2)–F(3)	2.34(3)
Mn–F(2)	2.05(2)		F(2)–F(5)	2.51(2)
Mn–F(6)	2.09(3)	×2	F(2)–F(6)	2.87(3)
Mn–F(5)	2.12(2)		F(2)–F(6)	2.95(2)
Mn–F(3)	2.29(2)		F(3)–F(4)	2.54(2)
Mn–F(4)	2.30(2)		F(3)–F(6)	2.96(3)
⟨Mn–F⟩ = 2.14			F(3)–F(6)	2.98(2)
			F(4)–F(6)	2.92(2)
Zr–F(6)	2.03(3)	×2	F(4)–F(6)	2.97(3)
Zr–F(4)	2.08(2)		F(5)–F(6)	2.86(3)
Zr–F(5)	2.10(1)		F(5)–F(6)	3.00(2)
Zr–F(1)	2.10(6)			
Zr–F(2)	2.11(2)			
Zr–F(3)	2.15(2)			
⟨Zr–F⟩ = 2.09				
F(2)^{ii}–Mn–F(4)^{ii}	131.8(9)		F(2)^{ii}–Mn–F(5)^{i}	164(1)
F(3)^{i}–Mn–F(5)^{i}	130.8(9)		F(3)^{i}–Mn–F(1)^{ii}	144(1)
F(4)^{ii}–Mn–F(1)^{ii}	149(1)		F(6)^{i}–Mn–F(6)^{iv}	167.8(7)
F(2)^{i}–Zr–F(4)^{i}	141.4(8)		F(2)^{i}–Zr–F(1)^{i}	146(1)
F(3)^{ii}–Zr–F(4)^{i}	152(1)		F(3)^{ii}–Zr–F(5)^{ii}	139.9(9)
F(6)^{ii}–Zr–F(6)^{iv}	174.2(6)		F(5)^{ii}–Zr–F(1)^{i}	141(1)

Note. For symmetry codes, see Table 6a.

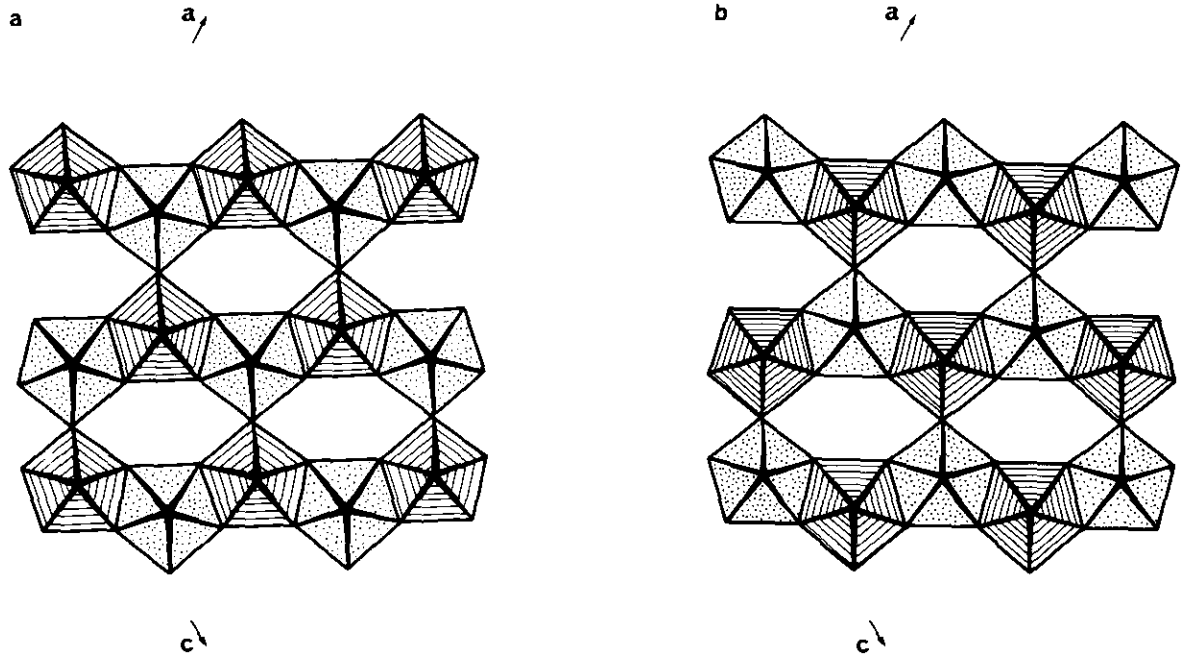

FIG. 2. Projection of the structure down [0 1 0]. (a) and (b) represent layers in y = 0.25 and 0.75, respectively. Dotted and hatched pentagonal bipyramids represent Zr and Mn polyhedra respectively.

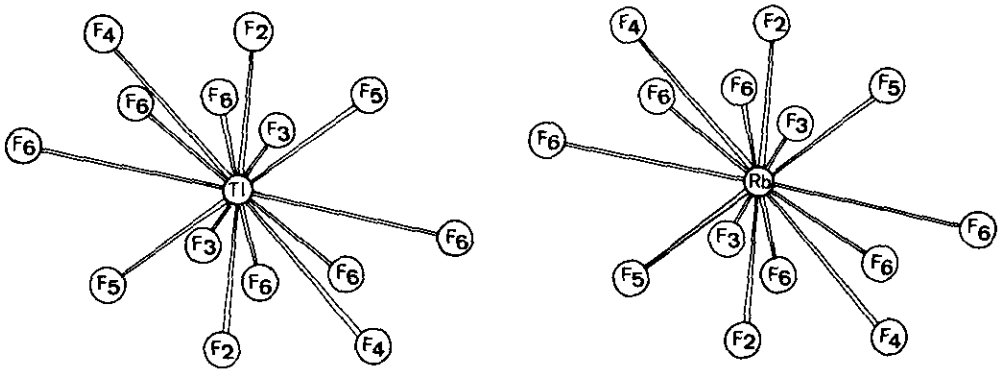

FIG. 3. Coordination polyhedra of Tl and Rb.

described as antiprismatic with a missing vertex, a mean Zr–F distance of 2.076 Å was observed. In most cases, the mean Zr–F distances observed for 7-coordinated zirconium lie in the 2.02–2.08 Å range (15).

As far as the Mn^{2+} ion is concerned, the 7-coordination is much more exceptional. This 7-coordination was pointed out only a few times in the fluorinated compounds, namely $MnCrF_5$ and its homologue α-$MnGaF_5$ (16), as well as $NaBa_2Mn_3F_{11}$ (17). In all of these examples, this 7-coordination is pentagonal bipyramidal.

Within the pentagonal bipyramids, the mean Mn–F distances in both Tl and Rb compounds, respectively 2.13 and 2.14 Å, are shorter than that found in $MnCrF_5$ (16), namely 2.22 Å.

This clearly shows that the MnF_7 pentagonal bipyramids exhibit a more regular geometry in the M^IMnZrF_7 fluorides than in $MnCrF_5$, since in the three cases the shortest Mn–F distance is equal to 2.02 Å, whereas the bond length ranges are 2.02–2.25, 2.02–2.30, and 2.02–2.43 Å, respectively.

Each pentagonal bipyramid surrounding the Zr^{4+} ions shares two edges and a corner involving equatorial vertices with three adjacent bipyramids of Mn^{2+} and vice versa, forming infinite layers (Fig. 2). Then, these layers by further vertex-sharing form a 3D structure. This 3D framework delimits channels parallel to the [0 1 0] direction within which the alkaline and the Tl^+ ions can be accomodated. Figure 3 displays both Tl and Rb coordination polyhedra.

In β-U_3O_8 (18) there are both distorted octahedral and pentagonal bipyramidal coordinations of the uranium atoms. This structure can be seen as constituted of a pentagonal bipyramidal network delimiting pseudohexagonal channels along the [0 1 0] direction in which are located chains of octahedra sharing apical vertices, these chains being connected to the network by edges. If these chains of octahedra are virtually removed, the remaining network is absolutely identical to the $(MnZRF_7)^-$ one in M^IMnZrF_7 compounds.

This pentagonal bipyramidal network is also quite similar to those encountered in both KIn_2F_7 (15) and β-KYb_2F_7 (19) structures. Figure 4 displays relationships between unit cells of KIn_2F_7, β-KYb_2F_7, and $TlMnZrF_7$.

MAGNETIC STUDY OF $TlMnZrF_7$

Figure 5 shows the applied magnetic field dependence of the magnetization of $TlMnZrF_7$ at different temperatures. At 4.2 K the saturation is reached in continuous magnetic field higher than 15 T. The saturation magnetization has been found to be equal to $4.92 \pm 0.1\ \mu_B$ in very good agreement with the $5\ \mu_B$ expected for the Mn^{2+} ion ($3d^5$). The magnetic susceptibility of the sample was deduced from the magnetization measurements performed at the lowest magnetic fields (0.4 to 0.6 T). Figure 6 exhibits the temperature dependence of the reciprocal

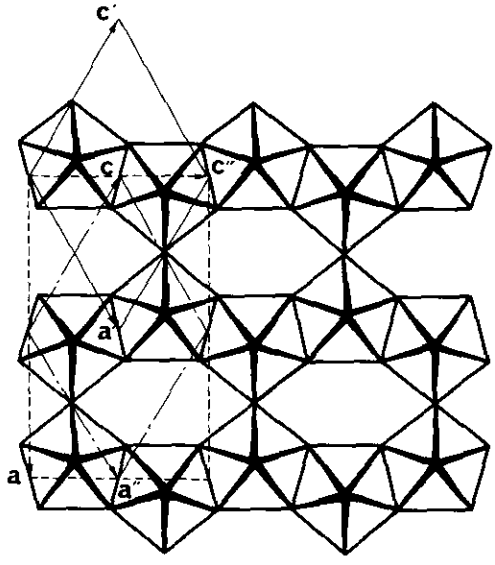

FIG. 4. Relationships between unit cells of KIn_2F_7 (a, c), β-KYb_2F_7 (a', c') and $TlMnZrF_7$ (a'', c'').

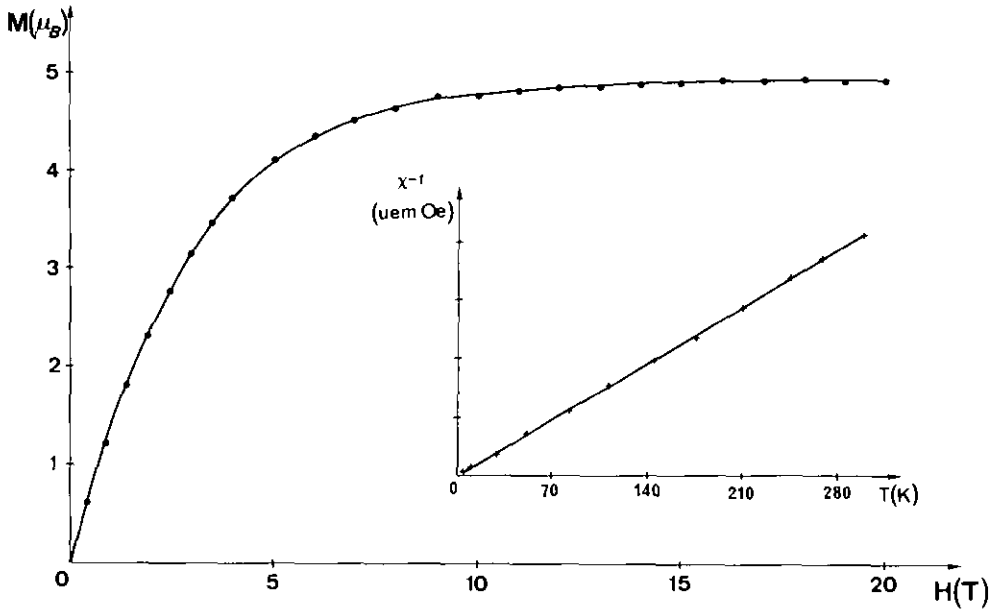

FIG. 5. Temperature and applied magnetic field dependence of the magnetization of TlMnZrF$_7$.

magnetic susceptibility. From a least squares fitting of the slope of this plot, an effective magnetic moment of 5.66 μ_B was obtained. This value slightly lower than the 5.92 μ_B theoritical one shows that the Mn^{2+} ions are in a high spin state. This thermal variation of the reciprocal magnetic susceptibility clearly shows that TlMnZrF$_7$ is paramagnetic over the 4.2–300 K temperature range. Moreover, this magnetic behavior is to be closely related to the three-dimensional Mn^{2+}–Zr^{4+} cationic order resulting in isolated Mn^{2+} ions. So no magnetic order can be expected, even at temperatures below 4.2 K.

CONCLUSION

The synthesis of M^IMnZrF$_7$ (M^I = Tl, Rb, NH$_4$, K) fluorides and the crystal structure determination of mem-

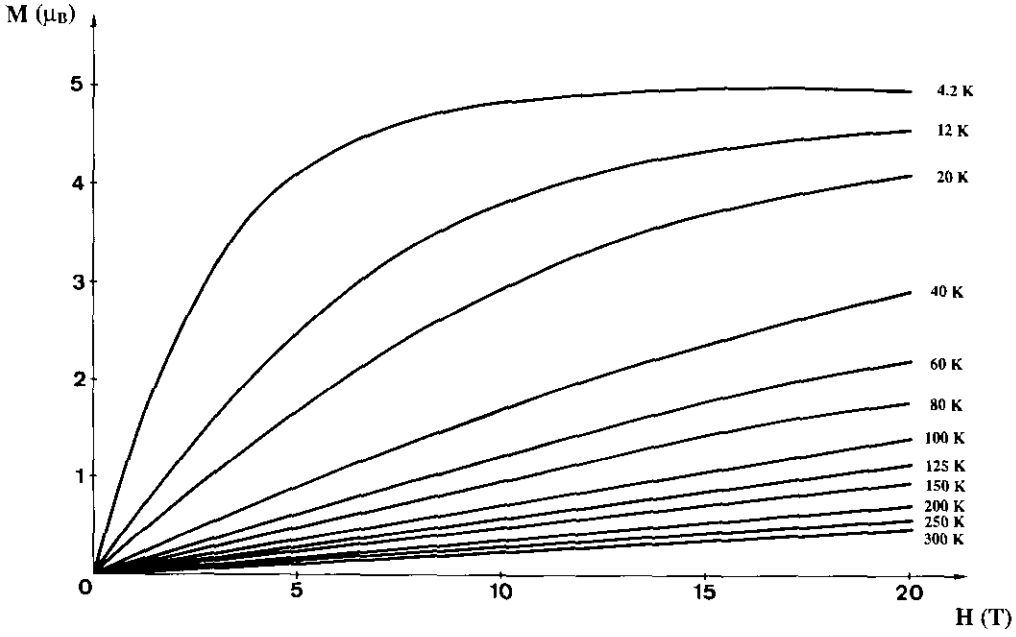

FIG. 6. Magnetic field dependence of the magnetization of TlMnZrF$_7$ at 4.2 K. The insert displays the temperature dependence of the reciprocal magnetic susceptibility.

bers of them have revealed a very original example of divalent manganese in 7-coordination with a pentagonal bipyramidal configuration. As this structural type may be closely related to both KIn_2F_7 and β-KYb_2F_7 structures by substituting the Mn^{2+}–Zr^{4+} couple for trivalent ions with appearance of a three-dimensional cationic order, it opens the route to the synthesis of new fluorides from archetypes within which trivalent cations of small size in 7-coordination are present.

REFERENCES

1. D. Avignant and J. C. Cousseins, C.R. *Acad. Sci. Ser. C* **274,** 631 (1972).
2. D. Avignant, I. Mansouri, R. Chevalier, and J. C. Cousseins, *J. Solid State Chem.* **38,** 121 (1981).
3. I. Mansouri and D. Avignant, *J. Solid State Chem.* **51,** 91 (1984).
4. D. Avignant, E. Caignol, R. Chevalier, and J. C. Cousseins, *Rev. Chim. Miner.* **24,** 391 (1987).
5. D. Avignant, E. Caignol, J. C. Cousseins, and I. Mansouri, *Eur. J. Solid State. Inorg. Chem.* **25,** 65 (1988).
6. E. Caignol, J. Metin, R. Chevalier, J. C. Cousseins, and D. Avignant, *Eur. J. Solid State. Inorg. Chem.* **25,** 399 (1988).
7. H. Holler, D. Babel, M. Samoüel, and A. de Kozak, *Eur. J. Solid State. Inorg. Chem.* **21,** 358 (1984).
8. J. C. Picoche, M. Guillot, and A. Marchand, *Physica B* **155,** 407 (1989).
9. J. C. Champarnaud-Mesjard and B. Frit, *Crystallogr. Sect. B* **33,** 3722 (1977).
10. "International Tables for X-Ray Crystallography," Vol. IV, Kynoch Press, Birmingham, 1968.
11. B. A. Frenz, *in* "Computing in Crystallography" (H. Shenk, R. Olthof-Hazekamp, H. Van Koningsveld, and G. C. Bassi, Eds.). Delft Univ. Press, Delft, The Netherlands, 1982.
12. R. D. Shannon and C. T. Prewitt, *Acta Crystallogr. Sect. B* **25,** 925 (1969).
13. J. P. Laval, B. Frit, and J. Lucas, *J. Solid State Chem.* **72,** 181 (1988).
14. G. Brunton, *Acta Crystallogr. Sect. B* **27,** 1944 (1971).
15. R. Coupe, D. Louer, J. Lucas, and A. J. Leonard, *J. Am. Ceram. Soc.* **66,** 523 (1983).
16. G. Ferey, Thesis Doctorat es Sciences, University P. and M. Curie 1977.
17. J. Darriet, M. Ducau, M. Feist, A. Tressaud, and P. Hagenmuller, *J. Solid State Chem.* **98,** 379 (1992).
18. B. O. Lopstra, *Acta Crystallogr. Sect. B* **26,** 656 (1970).
19. Y. Le Fur, S. Aleonard, M. F. Gorius, and M. T. Roux, *Acta Crystallogr. Sect. B* **38,** 1431 (1982).